

# Supplemental Material for J110057

November 15, 2017

## Further Observational Details

### Selection in SDSS-III BOSS of J110057

SDSS J110057.71-005304.5 was first detected by the ROSAT and appears in the All-Sky Survey Bright Source Catalogue [RASS-BSC; 6, 35]. J110057 was then imaged by the Sloan Digital Sky Survey (SDSS) and satisfied a number of spectroscopic targeting flags<sup>1</sup> making it a quasar target. A spectrum was obtained on MJD 51908 (Plate 277, Fiber 212) and the spectrum of a  $z = 0.378$  quasar was catalogued in the SDSS Early Data Release [28, 33]. The physical properties of J110057, derived from the MJD 51908 spectrum and using the methods in Shen et al. [30], are given in Table 1.

The second epoch spectrum is from the SDSS-III Baryon Oscillation Spectroscopic Survey [BOSS; 8] and shows the downturn at  $\lesssim 4300\text{\AA}$ . SDSS-III BOSS actively vetoed low- $z$  QSOs [27], and it was due to J110057 being selected as an ancillary target via a white dwarf program [14, 15] that a second spectral epoch was obtained. Since J110057 was not a BOSS QSO target, it is not subject to the “blue offset”, see Margala et al. [18].

A third epoch spectrum was obtained from the Palomar Hale 5m telescope using the DBSP instrument. Two exposures of 600s+300s were taken in good conditions. Features to note include the continuum straddling Mg II being blue in the 2017 spectrum, as it was for the SDSS spectrum in 2000, as opposed to red, as it was for the BOSS spectrum in 2010.

J110057 is in Data Release 3 (DR3) of the Dark Energy Camera Legacy Survey (DECaLS), where there are 8, 3 and 9 exposures in the  $g$ ,  $r$  and  $z$ -band respectively. The  $g$ - and  $r$ -band observations are separated by roughly a year, ( $56707 \leq g_{\text{MJD}} \leq 56727$  and  $56367 \leq r_{\text{MJD}} \leq 56367$ ). The  $z$ -band observations span almost 3 years ( $56383 \leq z_{\text{MJD}} \leq 57398$ ).

### Selection in NEOWISE-R of J110057

WISE W1 and W2 lightcurves for  $\sim 200,000$  SDSS spectroscopic quasars were obtained. These light curves span from the beginning of the WISE mission (2010 January) through the first-year of NEOWISE-R operations (2014 December). The W1/W2 light curves are obtained by performing forced photometry

<sup>1</sup>SERENDIP\_BLUE, ROSAT\_D, ROSAT\_C, ROSAT\_B, QSO\_SKIRT, ROSAT\_A, see Stoughton et al. [32] and Richards et al. [26] for flag descriptions.

Quantity	Value
SDSS name	J110057.71-005304.5
R.A. / deg	165.240463
Declination / deg	-0.884586
redshift, $z$	$0.3778 \pm 0.0003$
$M_i(z=2)$ / mag	-24.48
$\log(L_{\text{bol}}/\text{ergs}^{-1})$	$45.78 \pm 0.02$
$\log(M_{\text{BH}}/M_{\odot})$	$8.83 \pm 0.14$
Eddington ratio	0.070

Table 1: Physical properties of J110057 using the methods from Shen et al. [30].

at the locations of DECam-detected optical sources [17, 20, 21]. This forced photometry is performed on time-resolved unWISE coadds [17], each of which represents a stack of  $\sim 12$  exposures. A given sky location is observed by WISE for  $\sim 1$  day once every six months, which means that the forced photometry light curves typically have four coadd epochs available. Coadd epochs of a given object are separated by a minimum of six months and a maximum of four years. The coaddition removes the possibility of probing variability on  $\lesssim 1$  day time scales, but pushes  $\approx 1.4$  magnitudes deeper than individual exposures while removing virtually all single-exposure artifacts (e.g. cosmic rays and satellites).

Approximately  $\sim 30,000^2$  of the SDSS/BOSS quasars with W1/W2 light-curves available are “IR-bright”, in that they are above both the W1 and W2 single exposure thresholds and therefore detected at very high significance in the coadds. For this ensemble of objects, the typical variation in each quasar’s measured (W1-W2) color is 0.06 magnitudes. This includes statistical and systematic errors which are expected to contribute variations at the few hundredths of a magnitude level. The typical measured single-band scatter is 0.07 magnitudes in each of W1 and W2.

We undertook a search for outliers relative to these trends. Specifically, we selected objects with the following characteristics:

- Monotonic variation in both W1 and W2.
- W1 versus W2 flux correlation coefficient  $\geq 0.9$ .
- $> 0.5$  mag peak-to-peak variation in either W1 or W2.

This yields a sample of 248 sources. 31 of these are assumed to be blazars due to the presence of FIRST radio counterparts, and we discount them in the further analyses here. Another 22 are outside of the FIRST footprint, leaving 195 quasars in our IR-variable sample.

A link to our sample can be found here: `qso_pages_v01` and links to the catalogs are given here: `dr3_wise_lc_sample.fits.gz` and here: `dr3_wise_lc_sample.fits.gz`. The first catalog has 248 rows, which are the highly IR-variable sample of objects. The second catalog is the full 200 622 quasar sample quasars that have “good” WISE light curves available in DECaLS DR3. In each file, there are 3 extensions: the first extension are the WISE light curve summary metrics; the second extension the DECaLS DR3 data for each object, and the third extension, the SDSS data for each object. A full characterization of the typical mid-IR quasar variability will be presented separately.

## Additional Multiwavelength data for J110057

Checking the data archives we found there was no source within 30 arcsec in the VLA FIRST, i.e., at 21 cm radio frequencies for J110057. None of the *Hubble Space Telescope*, the *Spitzer Space Telescope* or the *Kepler* Mission has observed J110057. It is also not in the Hyper Suprime-Cam (HSC) Data Release 1 [5] footprint. There is the detection in ROSAT (which triggers using the 2nd all-sky survey (2RXS; Boller et al. 2016, A&A, 588, 103) as 2RXS J110058.1-005259 with 27.00 counts (count error 6.14) and a count rate =  $0.06 \pm 0.01$ . The NED gives J110057 as  $1.27 \pm 0.28 \times 10^{-12}$  erg/cm<sup>2</sup>/s in the 0.1-2.4 keV range (unabsorbed flux). J110057 is not in either *Chandra* or *XMM-Newton*.

## Further Model Details

In this section we discuss several models trying to explain the light curve and spectral behaviour of J110057. Ultimately, we are forced towards a model that combines a cooling front propagating in the accretion disk along with changes in the disk opacity.

### Scenario I: Obscuring Cloud model

We first explore the possibility that an obscuring cloud, or clouds, cause the observed light curve and spectral behaviour of J110057. In this scenario, one would require the obscuring cloud(s) to cross the

---

<sup>2</sup>NPR NOTE:: This number seems low to me; NPR to double check; can also triple check with Aaron

line of sight. In order to explain both the IR drop and broadline disappearance, one would also need the cloud(s) to block most of the inner disk such that the ionizing radiation could not impact on the BLR clouds or the torus for a period of months-years. Another requirement is an explanation of why the light curves ‘recover’ after a period of  $\sim 2500$  days (observed-frame); i.e., the light curves do not rapidly return to their original flux levels once the obscuring event is over.

Clouds should not typically infall; they need to lose angular momentum if they are drawn from a distribution with Keplerian orbits, and even if they do lose angular momentum, e.g., in a collision with approximately equal mass, they would likely be either destroyed or no longer coherent. Further issues arise, since the freefall timescales are,

$$t_{\text{ff}} \sim 100\text{yr} \left( \frac{r}{0.4\text{pc}} \right)^{3/2} \left( \frac{M}{10^8 M_{\odot}} \right)^{-1} \quad (1)$$

and Kelvin-Helmholtz instabilities would destroy the clouds within the cloud-crushing time, [e.g., 7, 13, 22, 31], given by

$$t_{\text{cc}} \sim 100\text{yr} \left( \frac{\rho_{\text{cloud}}/\rho_{\text{medium}}}{10^6} \right)^{1/2} \left( \frac{R_{\text{cloud}}}{4 \times 10^{10}\text{km}} \right) \left( \frac{v_{\text{rel}}}{10^4\text{km/s}} \right)^{-1} \quad (2)$$

Thus, even if clouds did infall, they would end up fragmented, which should pollute the inner disk (see below for this discussion applied to the circumstances in Guo et al. [12]).

The dust in the cloud is then well inside the dust sublimation radius

$$R_{\text{dust}} \approx 0.4\text{pc} \left( \frac{L}{10^{45}\text{erg/s}} \right)^{1/2} \left( \frac{T_{\text{sub}}}{1500\text{K}} \right)^{2.6} \quad (3)$$

and so the dust will be destroyed in the  $\sim 100$  year free-fall from the dust-sublimation region. Hence, one can not absorb the UV spectrum with dust, since it will have been sublimated well before it arrives at the inner disk.

Typical extinction profiles from clouds with hydrogen column densities of  $N_H \sim 10^{21} - 10^{22}\text{cm}^{-2}$  (comparable to the range expected for NLR-BLR cloud densities) are linear in  $1/\lambda$  with the  $2175 \text{ \AA}$  feature, [e.g., Figure 4 of 11], and not at all like the asymptotic drop off at  $1/\lambda = 3(\mu\text{m}^{-1}) = 1/300\text{nm}$  in Guo et al. [12] or in our 2010 spectrum. Note that in the extinction profiles in Gordon et al. [11], there is a local maximum near  $4.5 \sim 1/\lambda(\mu\text{m}^{-1})$ , implying  $\lambda \sim 0.2\mu\text{m}$  in these cloud extinction profiles. This could correspond to broadened  $\text{Ly}\alpha$  absorption; if this is broadened in a turbulent environment and combined with strong oxygen and carbon edges in a colder phase medium, it is possible to generate the falling off at  $1/(200\text{-}300\text{nm})$  in our 2010 spectrum (and Guo et al.’s spectrum). With all these considerations, we make a strong case that the behaviour observed in J110057 *cannot* be extinction due to a dusty cloud.

## Scenario II: Accretion Disk model

Having discounted an obscuring event as the explanation for J110057, we turn to an accretion disk model.

The early 2000s spectrum is well fit with a thin, Shakura & Sunyaev [29]  $\alpha$ -disk. The 2010 spectrum and the sharp fall-off at  $\sim 200 - 300\text{nm}$ , is not reproducible using a different temperature profile alone, even one where the entire inner disk (unphysically) vanishes. This is due to the width of the Planck function in wavelength space. For the same reasons, a gray absorber model with uniformly suppressed emission at small disk radii is also incapable of fitting our 2010 (or Guo et al.’s) spectrum. Wavelength dependent absorption, combined with a lower disk emissivity is required.

**MODEL ‘A’: SWITCHING STATES TO AN ADAF:** The broadband spectrum of NGC 1097 from Nemmen et al. [25] initially appears similar to the UV/optical 2010 spectrum of J110057. In Nemmen et al. [25, e.g., their Figure 4], there are disk model components that look similar to the fall-off at  $200\text{nm}$  observed in the J11057 2010 spectrum. This would involve a thin disk component extending from  $\sim 450r_g$  to the outer regions of the disk. Figure 4 in Nemmen et al. [25] shows the Multicolor Disk (MCD) blackbody-like model component from the thin disk at  $R > 450r_g$  (their long dashed line)

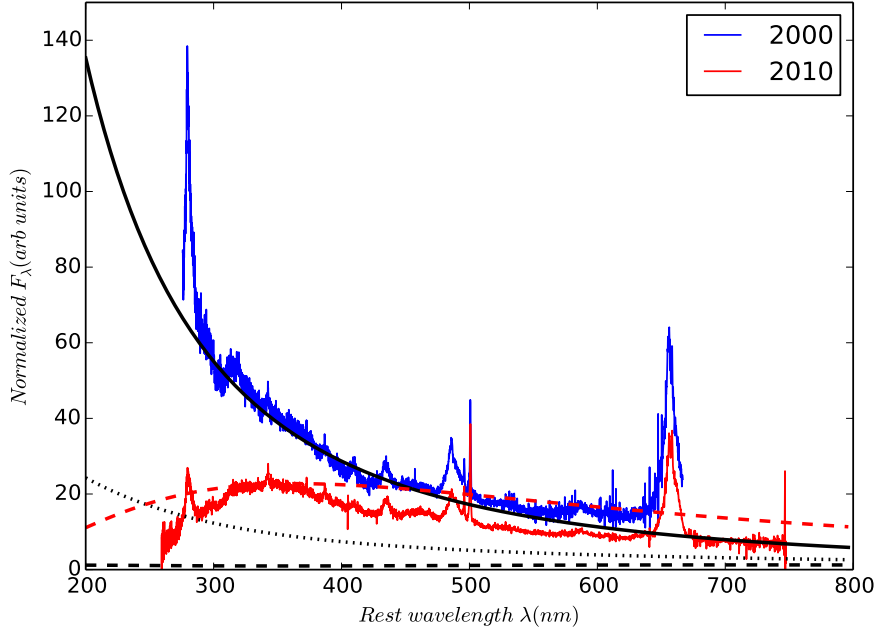


Figure 1: J110057 data (blue line 2000 spectrum; red line 2010 spectrum) and 4 models. Solid black line shows non-zero torque at ISCO [following 3]; dotted and dashed black lines show temperature suppression inside  $r_{\text{alt}} = 450r_g$ , such that the spectral flux is  $f_{\text{dep}} = 0.2$  or  $0.01$  (respectively) compared to a zero torque model; dashed red line shows zero flux inside  $r_{\text{alt}} = 150r_g$  and arbitrary normalization to match peak of 2010 spectrum. Note the poor fit due to the intrinsic width of the thermal peak.

dramatically decreasing at  $\sim 10^{15}\text{Hz}$  ( $\sim 300\text{nm}$ ). Nemmen et al. [25] model the disk region interior to this as an advection-dominated accretion flow (ADAF), at a power (in  $\nu L_\nu$ ), an order of magnitude lower than the MCD in the optical, but spanning from the X-ray to the far-IR.<sup>3</sup>

Can J110057 switch states from a thin disk quasar to an ADAF at small radii with the thin disk surviving at large radii? Assuming the transition happens due to an instability on the thermal timescale of the disk, then at large radii the thermal timescale is

$$t_{\text{th}} \sim 14 \text{ years} \left( \frac{\alpha}{0.03} \right)^{-1} \left( \frac{R}{450r_g} \right)^{3/2} \frac{r_g}{c} \quad (4)$$

and is too long given the observations. However, if the viscosity parameter  $\alpha$  increases to  $\alpha \approx 0.3$ , as suggested by King et al. [16], then the thermal timescale is  $t_{\text{th}} \sim 1.4 \text{ year}$  and the front timescale is

$$t_{\text{front}} \sim 10 \text{ years} \left( \frac{h/R}{0.05} \right)^{-1} \left( \frac{\alpha}{0.3} \right)^{-1} \left( \frac{R}{450r_g} \right)^{3/2} \frac{r_g}{c} \quad (5)$$

which is plausible, if there exists a very viscous disk and the effect propagates outwards on a timescale of  $\leq 10$  years from the inner disk. This would suppress the UV/X-ray emission from the RIAF (down by a few orders of magnitude from the intensity expected from a thin disk intensity) and explain the broadline behaviour. ADAF spectra are flat in  $\nu L_\nu$  Abramowicz & Fragile [1], Abramowicz et al. [2], Narayan et al. [24], and convective ADAFs rise towards X-ray energies. ADAFs exist at lower luminosity, where  $\varepsilon \sim 0.005$  for  $L = \varepsilon \dot{M} c^2$ , lower than the fiducial  $\varepsilon \sim 0.1$  for a classic thin disk luminosity.

However, suppressing the flux from the inner disk radii ( $\lesssim 450r_g$ ) in the low temperature thin disk model [3, 4, 9, 10, 23], by a factor of 20 would still not describe the 2010 spectrum. To restore the thin

<sup>3</sup>A change to a radiatively inefficient accretion flow (RIAF) is also possible in this model.

disk spectrum by 2016, the disk change has to propagate back inwards, most of the way to the ISCO and therefore  $t_{\text{front}}$  needs to be shorter. This requires  $h/R$  to be larger in Equation above, by a factor of  $\sim 2$ .

It is unclear what physical processes would trigger the change of state to an ADAF and then cool back down to a thin disk. However, more of an issue is that suppressing the MCD temperature profile inside a radius of  $R_{\text{alt}} = 450r_g$  leads to a collapse in the total flux compared to unperturbed disk. We show some example cases in 1. Clearly, these scenarios are difficult to reconcile with our data.

**MODEL ‘B’: PROPAGATING OF A COOLING FRONT:** An alternative model connected to the accretion disk is that a *cooling* front propagates through the thin disk. In order to reproduce the steep fall at  $\lambda \leq 200\text{nm}$  in the 2010 spectrum, a cool phase leads to absorption at short wavelengths.

Initially a modestly fat disk ( $h/R \sim 0.2$ ) with a modest  $\alpha$ , cools from the ISCO and propagates outward in a cooling front, collapsing the disk. As the hot disk ( $\sim 10^{5-6}\text{K}$ ) cools, it fragments into cooler clumps around  $\sim 10^4\text{K}$  [see e.g., 19]. The main coolants are resonance lines in carbon and oxygen [see e.g., Fig. 18 in 34]. The ionization energies for carbon and carbon are 11.26 and 13.61 eV, respectively, i.e.,  $\sim 100\text{nm}$ , and hence at wavelengths  $< 100\text{nm}$  the disk opacity will increase dramatically in an edge. However, the gas in the disk is both pressure, turbulent and Doppler broadened, so these ionization edges will manifest around  $100\text{nm}$  with decreasing opacity to shorter wavelengths as

$$\kappa \propto \rho T^{-1/2} \nu^{-3} \quad (6)$$

for Kramers’ opacities. This implies  $\kappa \propto \lambda^3$  at increasing wavelengths up to the ionization edge around  $100\text{nm}$ . These features will be blurred (by the broadening) and the ionization edges due to the C and O resonance lines in the cool phase of this disk will be span  $50 - 200\text{nm}$ , depressing the flux at these energies.

The 2010 spectrum in this model comes from a cooler disk plus the increased opacity at short wavelengths in the cooler phase. Heating occurs from the outside in, explaining the 2016 spectrum and asymmetric recovery in photometry. Since the optical continuum has been rising again since mid-2016, this leads to a prediction of a rise in hydrogen emission line flux in the next few months (2018). The infrared flux returns in 2021.

## Comparison with SDSS J2317+0005 from Guo et al. 2016

Figure 1 of Guo et al. (2016) shows a UV collapse in the quasar SDSS J231742.60+000535.1 (hereafter J2317+0005, with redshift  $z = 0.32$ ), similar to that of J110057. In Figure 2 we show the five SDSS/BOSS spectra from J110057 and J2317+0005 (top panel), and their ratios (bottom panel). The collapse in J2317+0005 happens in 23 days [Figure 2 of 12]; this object was observed by SDSS on MJD 52177 (normal) and then on MJD 52200. In the second epoch spectrum, there is a drop of 1.2 mag in the  $u$ -band and 0.5mag in  $g$ -band. The  $r, i, z$ -bands are all consistent with the earlier observation. J2317+0005 is observed with SDSS  $\sim$ a year later and  $(u, g, r, i, z)$  are all consistent with the earlier MJD 52177 spectrum. XMM-Newton spectra straddle this time period, from 2001 June 03 2001 November 28. Both x-ray spectra are consistent with no neutral absorption in the rest-frame. This implies the sight-line is clear on both of those dates. Guo et al. [12] also find that the IR does not significantly change and that the broad lines are consistent with being constant over time.

Guo et al. [12] discuss two scenarios to explain this behaviour: (i) an inner accretion disk change and (ii) an eclipse by an optically thick cloud. Guo et al. [12] note that in principle both models could explain the observation. In the inner accretion disk scenario, turning off the disk at  $r < 60r_g$  would explain the J2317+0005 spectra, though the detailed MCD fit is far from ideal, in much the same manner as for J11057. However, Guo et al. [12] find this explanation unconvincing since “quasars are not observed to flicker like this typically”. The second scenario is favoured based on the initial optical spectrum (23 days before the  $u$ -band dip) and the 2001 November x-ray spectrum (45 days after the  $u$ -band dip). For the reasons given above for J110057, and in particular with our infrared light curve data, we suggest  $\approx 45$  days is too short for an obscuration event, and hence suggest that the same initial cause (model B above: a cooling front propagating from the inner accretion disk) explains *both* the Guo et al. [12] spectrum and our 2010 spectrum. In the case of the Guo et al. [12] source, the fact that the IR and broad lines

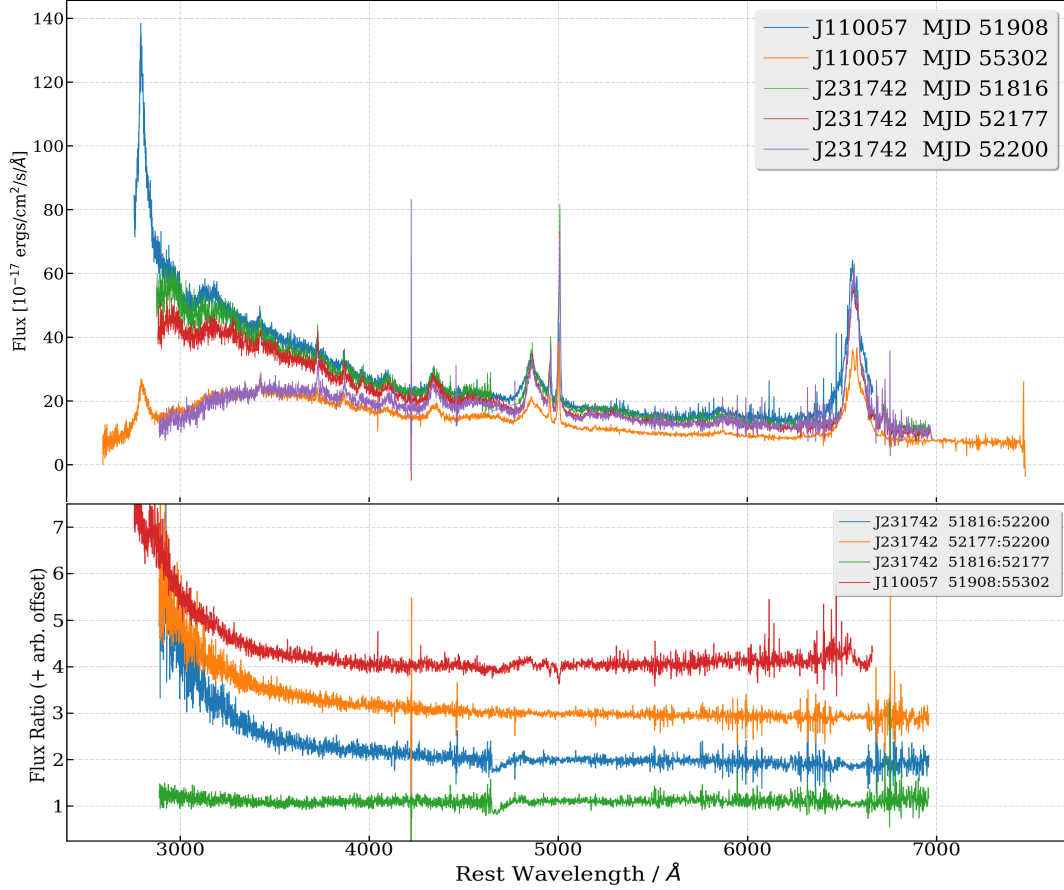


Figure 2: *Top*:: The five SDSS/BOSS spectra of J2317+0005 and J110057. The striking similarity between the two spectra downturned in the blue can be seen. *Bottom*:: The ratio of the different epoch spectra.

are unchanged implies that the temporary disk dimming is very short-lived. Therefore, in the case of Guo et al. [12], the restoring heating front must propagate outwards from the inner disk. This is unlike J110057 (model B above), where the restoring heating front must propagate inwards from the outer disk in order to explain the restoration of g-band before u-band and the long-term suppression of broad lines and IR.

## References

- [1] Abramowicz M. A., Fragile P. C., 2013, *Living Reviews in Relativity*, 16, 1
- [2] Abramowicz M. A., Igumenshchev I. V., Quataert E., Narayan R., 2002, *ApJ*, 565, 1101
- [3] Afshordi N., Paczyński B., 2003, *ApJ*, 592, 354
- [4] Agol E., Krolik J. H., 2000, *ApJ*, 528, 161
- [5] Aihara H., et al., 2017, *ArXiv e-prints*
- [6] Appenzeller I., et al., 1998, *ApJS*, 117, 319
- [7] Bae H.-J., Woo J.-H., 2016, *ApJ*, 828, 97
- [8] Dawson K., et al., 2013, *AJ*, 145, 10
- [9] Ford S., et al., 2018, in prep.

- [10] Gammie C. F., 1999, *ApJ Lett.*, 522, L57
- [11] Gordon K. D., Clayton G. C., Misselt K. A., Landolt A. U., Wolff M. J., 2003, *ApJ*, 594, 279
- [12] Guo H., et al., 2016, *ApJ*, 826, 186
- [13] Hopkins P. F., 2013, *MNRAS*, 428, 2840
- [14] Kepler S. O., et al., 2015, *MNRAS*, 446, 4078
- [15] Kepler S. O., et al., 2016, *MNRAS*, 455, 3413
- [16] King A. R., Pringle J. E., Livio M., 2007, *MNRAS*, 376, 1740
- [17] Lang D., 2014, *AJ*, 147, 108
- [18] Margala D., Kirkby D., Dawson K., Bailey S., Blanton M., Schneider D. P., 2016, *ApJ*, 831, 157
- [19] McCourt M., Oh S. P., O’Leary R. M., Madigan A.-M., 2016, *ArXiv e-prints*
- [20] Meisner A. M., Bromley B. C., Nugent P. E., Schlegel D. J., Kenyon S. J., Schlafly E. F., Dawson K. S., 2017, *AJ*, 153, 65
- [21] Meisner A. M., Lang D., Schlegel D. J., 2017, *AJ*, 154, 161
- [22] Nagakura H., Yamada S., 2008, *ApJ*, 689, 391
- [23] Narayan R., Kato S., Honma F., 1997, *ApJ*, 476, 49
- [24] Narayan R., Mahadevan R., Quataert E., 1998, in Abramowicz M. A., Björnsson G., Pringle J. E., eds, *Theory of Black Hole Accretion Disks Advection-dominated accretion around black holes*. pp 148–182
- [25] Nemmen R. S., Storchi-Bergmann T., Yuan F., Eracleous M., Terashima Y., Wilson A. S., 2006, *ApJ*, 643, 652
- [26] Richards G. T., et al., 2002, *AJ*, 123, 2945
- [27] Ross N. P., et al., 2012, *ApJS*, 199, 3
- [28] Schneider D. P., et al., 2002, *AJ*, 123, 567
- [29] Shakura N. I., Sunyaev R. A., 1973, *Astron. & Astrophys.*, 24, 337
- [30] Shen Y., et al., 2011, *ApJS*, 194, 45
- [31] Shiokawa H., Krolik J. H., Cheng R. M., Piran T., Noble S. C., 2015, *ApJ*, 804, 85
- [32] Stoughton C., et al., 2002a, *AJ*, 123, 485
- [33] Stoughton C., et al., 2002b, *AJ*, 123, 485
- [34] Sutherland R. S., Dopita M. A., 1993, *ApJS*, 88, 253
- [35] Voges W., et al., 1999, *Astron. & Astrophys.*, 349, 389